

## Merging energy-based design criteria and reliability-based methods: Exploring a new concept

Siddhartha Ghosh<sup>1,\*</sup>,<sup>†</sup>,<sup>‡</sup>,<sup>§</sup> and Kevin R. Collins<sup>2,‡</sup>,<sup>§</sup>

<sup>1</sup>*Department of Civil Engineering, Indian Institute of Technology Bombay, Powai, Mumbai 400076, India*

<sup>2</sup>*Department of Civil Engineering, Lawrence Technological University, Southfield, MI 48075, U.S.A.*

### SUMMARY

This paper examines the potential development of a probabilistic design methodology, considering hysteretic energy demand, within the framework of performance-based seismic design of buildings. This article does not propose specific energy-based criteria for design guidelines, but explores how such criteria can be treated from a probabilistic design perspective. Uniform hazard spectra for normalized hysteretic energy are constructed to characterize seismic demand at a specific site. These spectra, in combination with an equivalent systems methodology, are used to estimate hysteretic energy demand on real building structures. A design checking equation for a (hypothetical) probabilistic energy-based performance criterion is developed by accounting for the randomness of the earthquake phenomenon, the uncertainties associated with the equivalent system analysis technique, and with the site soil factor. The developed design checking equation itself is deterministic, and requires no probabilistic analysis for use. The application of the proposed equation is demonstrated by applying it to a trial design of a three-storey steel moment frame. The design checking equation represents a first step toward the development of a performance-based seismic design procedure based on energy criterion, and additional works needed to fully implement this are discussed in brief at the end of the paper. Copyright © 2006 John Wiley & Sons, Ltd.

Received 25 March 2004; Revised 14 April 2006; Accepted 14 April 2006

**KEY WORDS:** performance-based seismic design; energy-based design; probabilistic seismic hazard analysis; uniform hazard spectra; hysteretic energy demand; reliability-based design

\*Correspondence to: Siddhartha Ghosh, Department of Civil Engineering, Indian Institute of Technology Bombay, Powai, Mumbai 400076, India.

<sup>†</sup>E-mail: sghosh@civil.iitb.ac.in

<sup>‡</sup>E-mail: kevincollins@earthlink.net

<sup>§</sup>Assistant Professor.

Contract/grant sponsor: U.S. National Science Foundation; contract/grant number: CMS-9721452

## 1. INTRODUCTION

The Vision 2000 Committee, in its well-known report on the future of seismic design codes [1], proposed several different design approaches following a uniform conceptual framework for *performance-based seismic design* (PBSD). Of these procedures, the *general force/strength*, the *simplified force/strength* and the *prescriptive* approaches are modifications and enhancements of current practices using elastic design procedures, while the *comprehensive design*, the *displacement-based design* and the *energy-based design* approaches are potential design approaches needing development. The latter three procedures are targeted specifically for developing reliability-based design guidelines of the future. This paper explores a new concept of incorporating energy-based design criteria in the context of a reliability-based design methodology.

The need for an energy-based design methodology for earthquake resistant design of structures was recognized as early as the mid 1950s by Housner [2]. Over the past years, the state of the practice of seismic design of buildings has evolved from rudimentary force-based design methods to advanced displacement- or ductility-based methods, with probabilistic design gradually replacing the deterministic procedures. However, no detailed energy-based methodology has been proposed as yet. Researchers have stressed the necessity of an energy-based design methodology and the important role it would play in advanced seismic codes of the future [3–7].

In research over the last half century, different energy quantities, such as the *input energy* ( $E_i$ ), the *absorbed energy* ( $E_a$ ), the *hysteretic energy* ( $E_h$ ), etc., have been considered in seismic analysis of structures. Some of the studies have proposed input energy or absorbed energy for the purpose of seismic hazard estimation for an earthquake [4, 8], while others have used hysteretic energy for the same [6, 9]. However, many researchers have identified hysteretic energy demand or its 'equivalent parameters' as the demand parameters which are most closely correlated to seismic damage of structures [3, 5, 9]. This fact provides the motivation for the present work in which *normalized hysteretic energy* ( $E_N$ ) forms the basis of the energy-based design criterion. More complex damage parameters combining energy and displacement (ductility) demands, such as the Park and Ang damage index [10], may eventually prove to be better measures of damage in an energy-based methodology, but are not considered herein in an effort to keep the concepts and mathematics as simple as possible.

This paper explores one idea for incorporating energy-based design criteria into a probability-based code. The end product is not a detailed design procedure; instead, a design checking formula is developed that allows a designer to check whether or not a design satisfies a performance criterion stated in terms of hysteretic energy. The design checking formula is created by combining information from *uniform hazard spectra* (UHS) for normalized energy, an equivalent single-degree-of-freedom analysis methodology, a site soil factor, and a design factor calibrated using reliability theory. Each of these topics is discussed in the following sections. The application of the equation is demonstrated for a 3-storey steel moment frame. Finally, some strengths and weaknesses of the ideas outlined in the paper are highlighted, and future research needs are discussed.

## 2. UNIFORM HAZARD SPECTRA FOR NORMALIZED HYSTERETIC ENERGY

A uniform hazard spectrum is a form of response spectrum for which all the points on the curve correspond to a single probability of exceedance of the concerned hazard. For example, such a

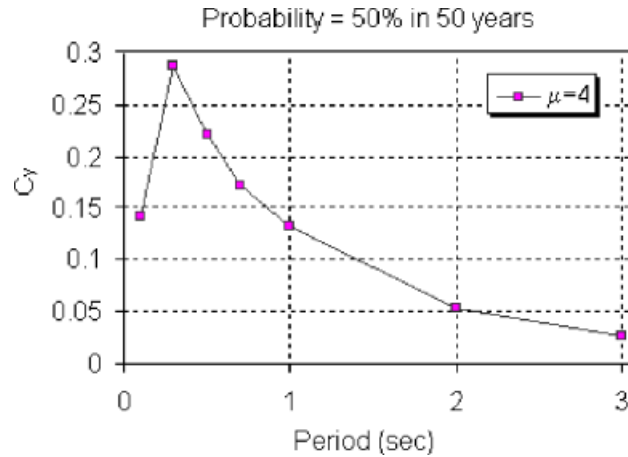


Figure 1. Uniform hazard spectrum for displacement ductility response ( $\mu = 4$ ).

spectrum can be constructed by obtaining the yield force coefficients ( $C_y$ , to be defined later) for single degree of freedom (SDOF) systems having different natural periods for a hazard described as ‘probability of exceeding a target ductility ( $\mu$ ) = 4.0 in 50 years is 50%’ (Figure 1). All the points in this curve correspond to that single hazard which is defined probabilistically.

To incorporate UHS in an energy-based design procedure, it is necessary to develop UHS curves that provide information on energy-based quantities or parameters. Different energy quantities can be obtained from the equation of motion for a viscous damped inelastic single degree of freedom system subjected to a ground motion excitation [11]. The governing equation can be written as

$$m\ddot{u} + c\dot{u} + f_s = -m\ddot{u}_g \quad (1)$$

where  $m$  is the mass of the system,  $c$  is damping coefficient,  $f_s$  is the restoring force of the inelastic spring,  $u$  is relative displacement of the mass, and  $\ddot{u}_g$  is ground acceleration. The hysteretic energy demand on the system is computed as

$$E_h = \int_0^u f_s du - \frac{f_s^2}{2k} \quad (2)$$

where  $k$  is the elastic stiffness.

Researchers have recommended various damage parameters based on hysteretic energy: some equivalent parameters, such as number of inelastic excursions or average rate of buildup of input energy [3, 5, 9, 12], and some combinations with other damage parameters, such as the Park and Ang damage index [10]. For a more detailed discussion on these damage parameters, the reader is referred to the work by Riddell and Garcia [7]. The focus of the current study is not to compare relative merits of all these damage parameters based on hysteretic energy. The proposed concept considers *normalized hysteretic energy* ( $E_N$ ) demand as the index for damage potential, which is defined as

$$E_N = \frac{E_h}{kd_y^2(1 - \alpha_k)} \quad (3)$$

where  $d_y$  is the yield displacement and  $\alpha_k$  is the strain-hardening stiffness ratio. Normalized hysteretic energy is chosen for this study because it keeps the mathematics relatively simple while still providing valuable information on energy demand and damage. This normalized hysteretic energy, unlike the actual hysteretic energy, is a non-dimensional quantity, so it is convenient for design application.

An elastic–perfectly plastic SDOF oscillator with viscous damping is used for generating the UHS presented here. The response of such a system to ground motions can be obtained following Equation (1) and its derivatives. Lack of any strain-hardening ( $\alpha_k = 0$ ) simplifies the expression for  $E_N$  to

$$E_N = \frac{E_h}{kd_y^2} \quad (4)$$

‘P-delta’ or secondary moment effects are not considered for the oscillator. It is also assumed that neither strength nor stiffness degradation occurs during subsequent displacement cycles. A damping factor ( $\zeta$ ) of 0.05 is assigned to the oscillator for all analyses.

The UHS are constructed for a location near Los Angeles, CA, at the geographical location of 118° West and 34° North. A set of 1292 simulated ground motion records was generated for the site by Collins [13, 14]. This set of ground motion records is used in the current research for constructing UHS for normalized hysteretic energy. The site soil is classified as Soil Class S<sub>2</sub> (‘deep cohesionless or stiff clay conditions’) in the 1992 NEHRP classification scheme [15]. The oscillator is analysed for a range of yield force values. These yield force values are normalized to define yield force coefficient,  $C_y$ .  $C_y$  is defined as the ratio of the spring force when  $d = d_y$  to the weight of the oscillator. Mathematically, it is expressed as

$$C_y = \frac{F_y}{W} = \omega_n^2 \frac{d_y}{g} \quad (5)$$

where  $F_y$  is spring force at  $d_y$ ,  $W$  is the weight of the oscillator, and  $\omega_n$  is the natural frequency of the system. This non-dimensional parameter  $C_y$  can be treated as a representation of the ‘yield strength’ of the system.

Non-linear time history analyses are carried out for all 1292 simulated earthquakes at discrete values of  $C_y$  and period  $T$ , and the maximum  $E_N$  is obtained for each one [16]. From the response statistics, exceedance probabilities for several target values of  $E_N$  (3, 4, 5, 10, 30, and 50) are calculated. These results are used to estimate values of  $C_y$ , at each period  $T$ , for which the probability of exceeding a target  $E_N$  has a specific value (for example, 10% in 50 years). Plotting these  $C_y$  values against period  $T$  gives a UHS for a specified  $E_N$  and target probability ( $p_t$ ). A uniform hazard spectra plot usually contains several of such curves with some commonality; for example, all the hazard curves may correspond to a fixed value of  $E_N$  but different probabilities of exceedance, and *vice versa*. Figures 2 and 3 show samples of both kinds of UHS.

Any point on these uniform hazard curves basically illustrates a mathematical expression of conditional probability similar to

$$P(E_N > E_{Nt} \text{ given } C_y) = p_t \quad (6)$$

where the subscript  $t$  refers to a target value of the parameter. Based on the statistics of the exceedance probabilities, periods, and target normalized hysteretic energy quantities, an empirical function of  $C_y$  describing this annual probability of exceeding a target value of  $E_N$  is determined.

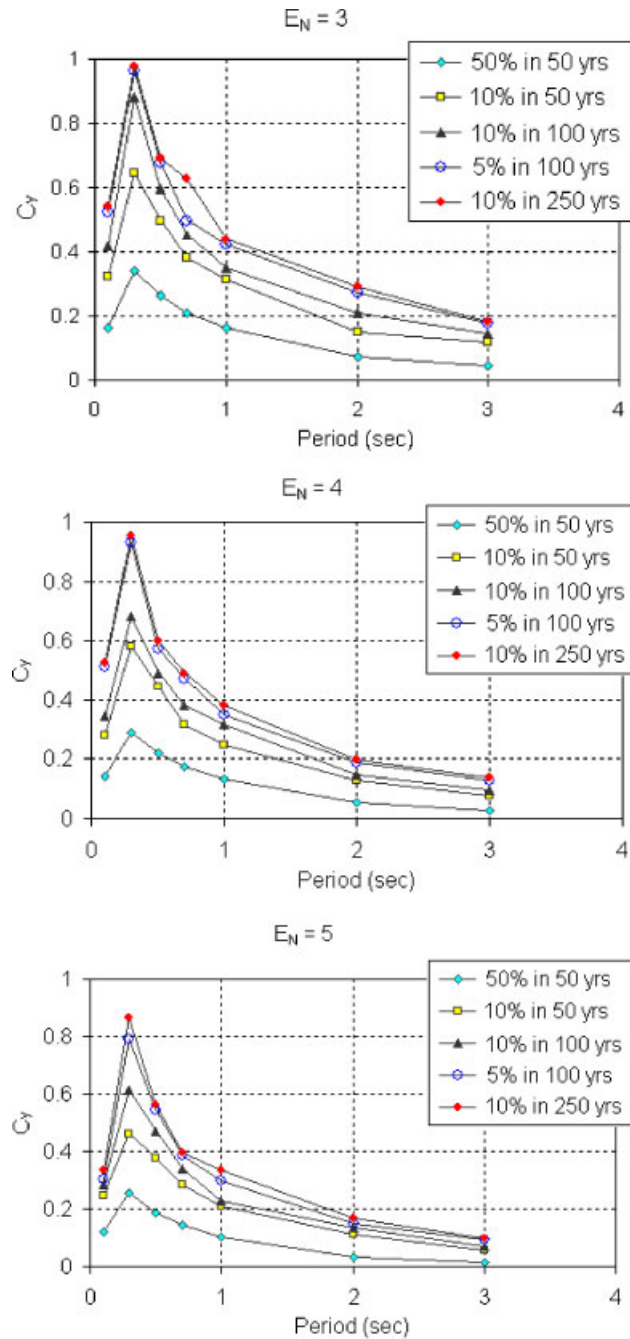


Figure 2. Uniform hazard spectra for  $E_N$ . Each plot presents the variation in  $C_y$  with period for a fixed  $E_N$  and different  $p_t$ .

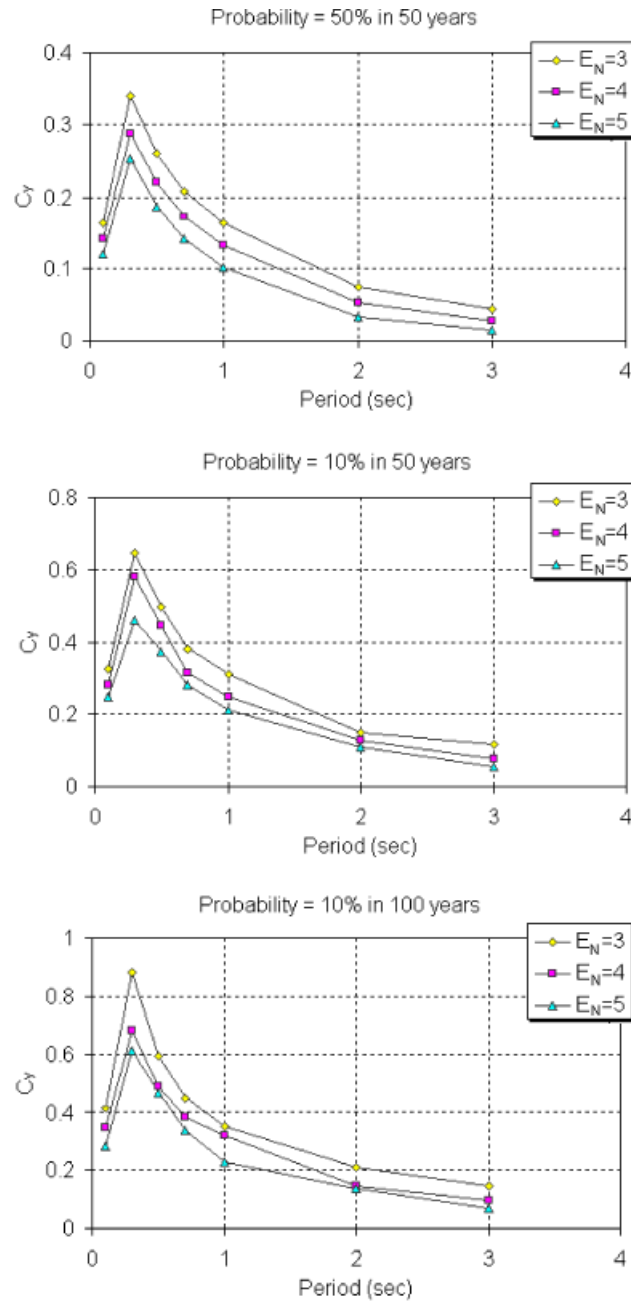


Figure 3. Uniform hazard spectra for  $E_N$ . Each plot presents the variation in  $C_T$  with period for a fixed  $p_t$  and different  $E_N$ .

Of the several empirical models investigated, the model which seems to provide the best fit overall is of the form

$$P(E_N > E_{Nt} \text{ given } C_y) = \exp\{-a(C_y)^b\} \quad (7)$$

Values of function parameters  $a$  and  $b$  are tabulated for each period and target energy quantity in Table I. Figure 4 compares the exceedance probabilities from the simulation study with the probabilities predicted by the empirical function for  $T = 0.3$  second and  $E_{Nt} = 4$ .

From these uniform hazard energy spectra, one can determine the required yield force coefficient ( $C_y$ ) for a SDOF system (whose  $T$  is known) at a certain location, so that the hysteretic energy demand can be limited to some desired level (defined in terms of  $E_{Nt}$  and  $p_t$ ). It is observed that for a fixed  $E_{Nt}$  and period, the probability of exceeding the  $E_{Nt}$  decreases as the required yield force coefficient increases. This is significant from a design perspective because it supports the intuitive notion that stronger structures should have lower hysteretic energy demands. Also, to maintain the same probability of exceedance for two target energy quantities  $E_{N1}$  and  $E_{N2}$  with  $E_{N2} > E_{N1}$ , the required  $C_y$  for  $E_{N1}$  has to be larger than that for  $E_{N2}$ . This is a very important observation for the purposes of developing design checking equations, because it allows designers

Table I. Values of function parameters  $a$  and  $b$  for different  $T$  and  $E_{Nt}$ .

$E_{Nt}$	$T = 0.1$ s		$T = 0.3$ s		$T = 0.5$ s		$T = 0.7$ s		$T = 1.0$ s		$T = 2.0$ s		$T = 3.0$ s	
	$a$	$b$												
3	9.30	0.33	7.60	0.35	8.3	0.38	9.10	0.43	10.6	0.45	12.7	0.40	14.5	0.37
4	9.30	0.28	7.70	0.35	8.9	0.35	9.40	0.39	11.5	0.45	12.9	0.35	15.5	0.35
5	9.50	0.27	8.00	0.33	9.5	0.38	11.0	0.46	11.0	0.35	14.3	0.35	15.2	0.30
10	9.80	0.33	8.80	0.31	10.1	0.38	12.8	0.52	14.0	0.48	20.0	0.48	23.5	0.45
30	10.6	0.34	9.90	0.32	12.8	0.43	16.0	0.51	18.0	0.49	26.0	0.48	32.0	0.46
50	11.2	0.36	10.8	0.35	14.2	0.45	16.3	0.45	18.2	0.45	31.5	0.49	46.0	0.51

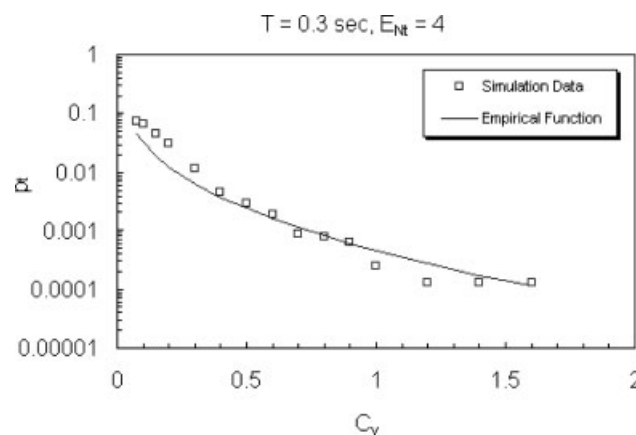


Figure 4. Comparison of  $p_t$  for the simulation data with the probabilities predicted by the empirical function (Equation (7)) for  $T = 0.3$  s and  $E_{Nt} = 4$ .

to interpret hysteretic energy-based criterion in terms of commonly used parameters such as the yield force coefficient or the yield displacement.

The generated UHS provide information on the energy demand only for SDOF systems. The following section discusses how an ‘equivalent system methodology’ can be used in combination with these UHS to estimate the energy demand on MDOF systems, such as buildings.

### 3. EQUIVALENT SYSTEM METHODOLOGY

The concept of an ‘equivalent’ (or ‘generalized’) SDOF model of a MDOF structure is nothing new. Alternative methods for this purpose have been proposed over the years [13, 14, 17–20]. An equivalent single degree of freedom (ESDOF) system is a simplistic representation of an actual MDOF structure, based on properties of the real structure, such that the ESDOF system is capable of representing certain response(s) of the MDOF structure. Many previous applications of ESDOF techniques have focused on prediction of displacement quantities. One of the goals of this research is to determine if an equivalent system can be used for estimating energy demand on the original structure.

This study considers an ESDOF methodology based on non-linear static pushover analysis of the MDOF system, and is a variant of the method proposed by Qi and Moehle [17] and used by Collins [13]. The static force–displacement diagram obtained from the pushover analysis provides a measure of the strain energy and work capacity of the structure and provides a convenient (albeit approximate) method of visualizing the non-linear inelastic problem [21].

The formulation of a generalized or equivalent system starts from the dynamic response of a two-dimensional MDOF cantilever-type structure subjected to horizontal base motion

$$[M]\{\ddot{u}\} + [C]\{\dot{u}\} + \{R\} = -[M]\{1\}\ddot{u}_g \quad (8)$$

where  $[M]$  is the mass matrix (assumed to be diagonal),  $\{u\}$  or  $\{u(t)\}$  is the lateral displacement vector,  $[C]$  is the damping matrix, and  $\{R\}$  or  $\{R(t)\}$  is the restoring force vector.

The generalized system replaces the displacement vector,  $\{u(t)\}$ , with a single displacement, for example the roof displacement,  $D(t)$ , and introduces a time-invariant displacement profile or shape vector,  $\{\Phi_1\}$ . The shape vector  $\{\Phi_1\}$  is selected here based on the pushover analysis of the MDOF structure. The variation of base shear ( $V$ ) with generalized displacement ( $D$ ) during a static non-linear pushover analysis can be monitored and Figure 5 shows an example of such a  $V$  versus  $D$  plot, or ‘pushover plot’, for non-linear pushover analysis. In general, the relationship between  $V$  and  $D$  can be represented mathematically as

$$V = KG(D) \quad (9)$$

where  $K$  is the initial slope of the pushover curve and  $G$  is the scalar mathematical function of  $D$  describing the shape of the curve. It can be shown [13, 16] that Equation (8) can be reduced to

$$M^*\ddot{D} + C^*\dot{D} + K^*G(D) = -L^*\ddot{u}_g \quad (10)$$

or, after dividing by  $M^*$

$$\ddot{D} + 2\xi(\omega^*)\dot{D} + (\omega^*)^2G(D) = -P^*\ddot{u}_g \quad (11)$$

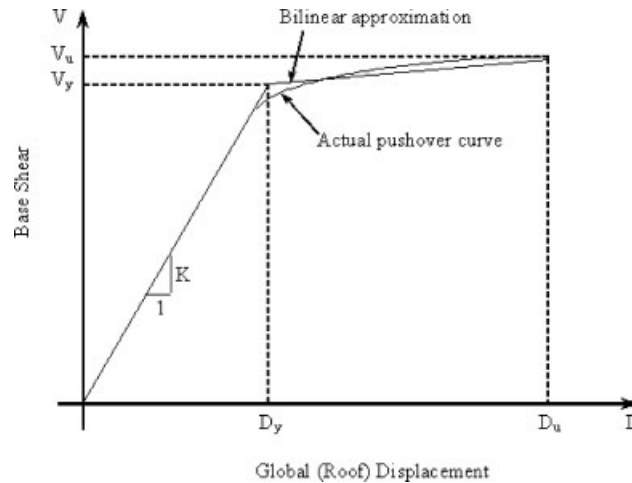


Figure 5. Sample of a  $V$  versus  $D$  plot based on non-linear static pushover analysis.

where  $M^* = \{\Phi_2\}^T [M] \{\Phi_1\}$ ,  $C^* = \{\Phi_2\}^T [C] \{\Phi_1\}$ ,  $K^* = K \{\Phi_2\}^T \{f\}$ ,  $L^* = \{\Phi_2\}^T [M] \{1\}$ ,  $P^* = L^* / M^*$ ,  $(\omega^*)^2 = K^* / M^*$ ,  $C^* / M^* = 2\zeta\omega^*$ ,  $\{\Phi_2\}$  is a premultiplying vector of choice, and  $\{f\}$  is the lateral force vector for pushover analysis. Equation (11) can be interpreted as the equation of motion of a SDOF oscillator with linear elastic frequency  $\omega^*$  and damping ratio  $\zeta$ .

In this paper, the vector  $\{\Phi_2\}$  is chosen to be  $\{\Phi_1\}$ . This is consistent with the equivalent SDOF equation derived using the principle of virtual work [22]. This formulation of ESDOF system is referred to as the *virtual work formulation* in this study. Alternate formulations have been discussed by Collins [13] and Ghosh [16].

In order to evaluate how well the proposed equivalent system methodologies predict energy demands, three two-dimensional steel moment frames are chosen for analysis. Hysteretic energy dissipation under different ground motion scenarios is considered for both the MDOF models of these frames and their ESDOF counterparts. The validity of proposed ESDOF models are tested by comparing these two sets of energy outputs.

The buildings considered for this study are the three-, nine- and twenty-storey 'Pre-Northridge' design steel moment frame buildings considered for the SAC joint venture [23]. The North-South frames of each building are considered for this study. Figure 6 shows the basic layout of these frames. Individual member sizes and other details can be found from other sources [16, 23] and are not reproduced here. These frames are chosen because they represent realistic designs of steel moment resisting frames. The computer program RAM Perform-2D [24] is used to perform non-linear static pushover analyses and also to perform the non-linear dynamic analyses for several selected ground motions. Gravity load effects on a frame are considered, while 'P-delta' effects, flexibility of joint panel zones, and stiffness contribution from gravity-frame members are not considered for analyses. Members of the moment frame are considered to be elastic-perfectly plastic. Actual (plastic) capacities of sections, instead of factored (design) capacities, are used for modelling. Rayleigh damping [11] is assumed for dynamic analysis. The mass proportional and the stiffness proportional damping coefficients are obtained by adopting a modal damping factor ( $\xi$ ) of 0.05 for the first and second modes.

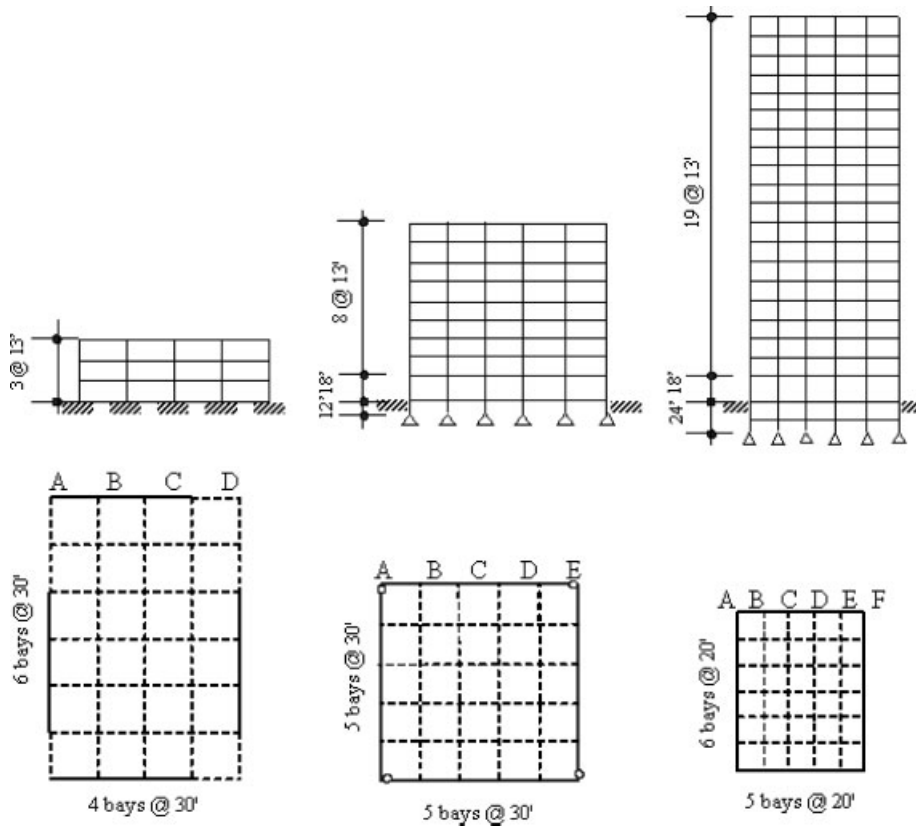


Figure 6. Elevations and floor plans (showing layouts of moment resisting frames in unbroken lines) of SAC buildings; 3-, 9- and 20-storey from left to right (1 ft = 0.305 m).

A total of 28 ground motions, 18 real earthquakes and 10 simulated, are considered for the comparison of hysteretic energy values of MDOF and ESDOF systems. The 10 simulated records are selected from the set of 1292 used to generate the UHS. The 18 real records include recordings from Parkfield '66, Landers '92, Northridge '94, Kobe '95, and Chi-Chi '99 earthquakes. Information on this set of ground motions can be found in the work by Ghosh [16].

For the pushover analyses, a lateral load distribution  $\{f\}$  as recommended in the Uniform Building Code [25] is used. A pushover analysis is carried out up to a global drift ( $\Delta$ ) of 2.5%, and the equivalent system parameters (yield displacement, yield base shear, etc.) are obtained by approximating the pushover curve by an elastic-perfectly plastic curve as shown in Figure 5. The approximate bilinear curve is assumed to have the same linear elastic stiffness and area under the curve as the pushover curve.  $\{\Phi_1\}$  is obtained from the displacement profile at 1% global drift. As noted earlier,  $\{\Phi_2\} = \{\Phi_1\}$  for the results presented herein.

For each frame, maximum hysteretic energy demand is obtained for each of the 28 ground motion scenarios and is compared with energy demands on the actual MDOF model. Information on the comparison between the MDOF response and the ESDOF model are illustrated using scatterplots (Figure 7). Results for each frame are presented separately. In each plot, a data point

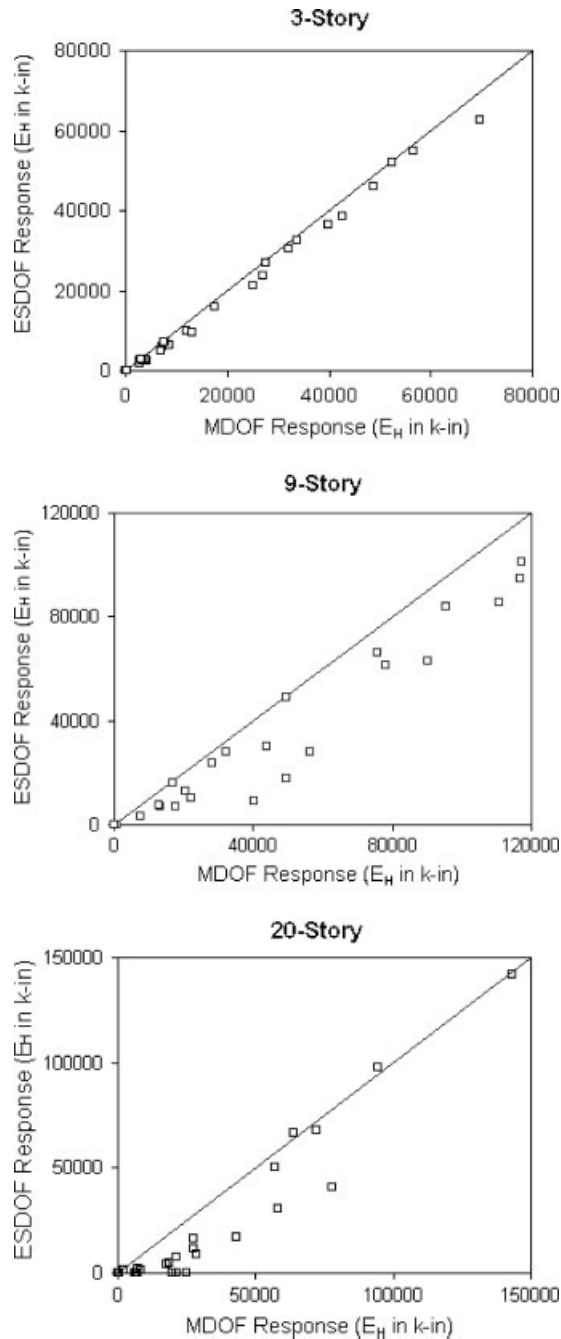


Figure 7. Scatterplots comparing maximum hysteretic energy responses of MDOF and ESDOF systems for the 3-, 9- and 20-storey frame (1 k-in = 0.113 kNm).

represents a comparison of the MDOF and the ESDOF responses for a single earthquake. The diagonal line across scatterplots represents the ideal ESDOF response, which is exactly the same as the MDOF response.

ESDOF parameters  $K^*$  and  $D_y^*$  (yield displacement of the equivalent system) are used for the normalization of the hysteretic energy ( $E_H$ ) for both the MDOF and ESDOF systems. The normalized hysteretic energy,  $E_N$ , is defined as

$$E_N = \frac{E_H}{K^*(D_y^*)^2} \quad (12)$$

This normalization scheme is adopted so that the uniform hazard spectra for normalized hysteretic energy can be used for the ESDOF systems. For a constant ductility, this  $E_N$  is directly proportional to the hysteretic energy dissipated in one full hysteresis loop for an elastic–perfectly plastic system.

The trend of overestimation or underestimation by the ESDOF model is analysed through bias factor statistics, where the bias factor is defined as the ratio of the MDOF system response to the ESDOF system response for a particular earthquake. The bias factor ( $N$ ) for this normalized hysteretic energy ( $E_N$ ) is defined as

$$N = \frac{E_N \text{ for MDOF}}{E_N \text{ for ESDOF}} = \frac{E_H \text{ for MDOF}}{E_H \text{ for ESDOF}} \quad (13)$$

The bias statistics for the data presented in Figure 7 are shown in Table II. Results for the three-storey frame are very close to the diagonal line (and mean bias factor is close to 1 with low coefficient of variation), which signifies that the ESDOF model can predict the energy demand on this frame very well. For the nine- and twenty-storey frames, points on the scatterplot fall below the diagonal line because MDOF demands are larger than ESDOF demands. Hence, we also get mean bias factors much higher than 1. A lower-bound cut-off value for  $E_N$  is set arbitrarily in order to discard earthquake records for which the hysteretic energy response is very low. All the earthquakes resulting in a demand less than  $E_N = 0.1$  for either the MDOF response or the ESDOF response are neglected for the study of bias statistics. This lower limit is uniform for all the frames considered for the validation of ESDOF method. A design procedure based on hysteretic energy-based criterion is not intended for cases where a very small amount of plasticity is involved. A lower limit of  $E_N$  eliminates only those cases for which a hysteretic energy-based design is not needed.

After this elimination, the numbers of ground motion records utilized for statistical analysis are 26, 23 and 15 for the three-, nine- and twenty-storey frames, respectively. A larger sample would produce more reliable statistics; however, the goal of this study is to illustrate how such

Table II. Bias statistics of  $E_N$  (SD = standard deviation, CoV = coefficient of variation).

	3-Storey bias	9-Storey bias	20-Storey bias
Mean	1.19	1.70	2.27
SD	0.164	0.793	1.23
CoV	0.137	0.467	0.542
Maximum	1.66	4.44	4.74
Minimum	1.01	1.01	0.961

information can be effectively used for probabilistic design. Keeping this in mind, this study proceeds to modelling of site soil effects and uncertainty analyses, which show how the ESDOF bias information is incorporated in developing a design checking methodology.

#### 4. MODELLING OF SITE SOIL EFFECTS

Modern seismic design provisions take care of the site soil effect by incorporating a scale factor, known as the *site coefficient* or the *site soil factor*. Based on conditions of the soil on which the structure is built, this factor is applied to the ground motion parameter under consideration (e.g. pseudo spectral acceleration).

The present study adopts a site classification based on the mean shear wave velocity in the near-surface soil at the site, following classification methods proposed in previous works [13, 26, 27]. Based on regression analysis of data recorded at 35 free-field sites after the 1989 Loma Prieta earthquake, Borcherdt [26, 27] developed the following equation for site soil factor:

$$F = \left( \frac{v_{\text{ref}}}{v_{\text{site}}} \right)^m \quad (14)$$

where  $F$  is the site soil factor,  $v_{\text{ref}}$  and  $v_{\text{site}}$  are the mean shear wave velocities for the reference soil condition and the actual site soil condition, respectively, and  $m$  is a regression parameter. The value of this regression parameter changes according to the fundamental period of the structure. The short period range covers periods from 0.1 second up to about 0.4–0.5 s, and the mid-period range includes periods over 0.4 up to 2.0 s. Based on the analysed data, values of  $m$  for short and mid-period ranges are 0.35 and 0.65, respectively. The parameter  $m$  may also depend on the intensity of the ground motion, but the dependence is neglected herein.

#### 5. ANALYSIS OF UNCERTAINTY

Three significant sources of uncertainty in seismic design of buildings are: the inherent uncertainty in the earthquake's occurrence time and damage potential, the uncertainty in predicting the site soil effects on ground motion, and the approximations involved in creating a model of the structure. The inherent uncertainty in the earthquake can be accounted for by using UHS as discussed earlier in Section 2. This section discusses the probabilistic methods used to quantify the two other sources of uncertainty: the site soil effects and the equivalent system methodology.

For probability analysis, Collins [13] showed that site soil factor  $F$  can be reasonably modelled using a lognormal distribution with a standard error of  $\log_{10} F$ , or  $\sigma_{\log F}$ , being about 0.21 for the short period range, and 0.18 for the mid-period range. Based on Equation (14), median values of  $F$  can be obtained for a variety of site classes. This distribution information, considering  $v_{\text{ref}} = 540$  m/s for the reference soil condition, is used later for calibrating design factors for different site conditions.

The uncertainty in prediction of the MDOF response using equivalent systems is accounted for through a bias factor,  $N$  (Equation (13)). Table II provides the results of bias data analysis for the *virtual work formulation* for different building frames. This bias information is used to come up with an empirical distribution model for the bias factor.

Table III. Performance of different trial distributions for bias factor ( $N$ ) in Kolmogorov–Smirnov Test ( $D_n^{0.05}$  = critical value of  $D_n$  at 5% significance level).

	Actual	Normal	Lognormal	Gamma	Extreme type I	Extreme type II
3-storey frame, $n_s = 26$ , $D_n^{0.05} = 0.264$ , $D_n^{0.01} = 0.313$						
Mean	1.19	1.19	1.19	1.21	1.19	1.20
SD	0.164	0.164	0.164	0.154	0.149	0.165
$D_n$		0.212	0.197	0.245	0.174	0.160
9-storey frame, $n_s = 23$ , $D_n^{0.05} = 0.278$ , $D_n^{0.01} = 0.236$						
Mean	1.70	1.70	1.70	1.71	1.69	1.70
SD	0.793	0.793	0.793	0.668	0.806	0.796
$D_n$		0.193	0.169	0.187	0.190	0.184
20-storey frame, $n_s = 15$ , $D_n^{0.05} = 0.34$ , $D_n^{0.01} = 0.40$						
Mean	2.27	2.27	2.27	2.27	2.15	2.44
SD	1.23	1.23	1.23	1.23	1.22	4.20
$D_n$		0.155	0.171	0.164	0.140	0.175

Table IV. Distribution parameters for the lognormal distribution of  $\sqrt{N}$ .

	Mean ( $\mu_{\sqrt{N}}$ )	SD ( $\sigma_{\sqrt{N}}$ )
3-storey	1.09	0.065
9-storey	1.26	0.192
20-storey	1.46	0.361

Several standard distributions are tried in order to fit the raw data and these distributions are: *Normal*, *Lognormal*, *Gamma*, *Extreme Type I*, and *Extreme Type II*. In order to select the best fit for all the three different frames a *Kolmogorov–Smirnov test* (K–S test) [28] is performed for each of the distributions. Table III shows how the different distributions perform in *K–S test* for three frames. Based on its overall low values in discrepancy ( $D_n$ ), and having the same mean and standard deviation as the raw data, the lognormal distribution is preferred over the other four distributions tested here. This distribution is acceptable at significance levels ( $\alpha_{\text{sig}}$ ) of 1% and 5%. As will be shown later, the choice of the lognormal distribution also simplifies the probability analysis.

Distribution information for  $\sqrt{N}$  is used later in the development of the design checking equation (Section 6). Distribution parameters for  $\sqrt{N}$  can be obtained from the distribution of  $N$ ; since  $N$  is lognormally distributed,  $\sqrt{N}$  will also be lognormally distributed. The distribution information for  $\sqrt{N}$  is provided in Table IV.

## 6. DESIGN CHECKING EQUATION

The purpose of the present research is to explore a prospective hysteretic energy-based design concept for real multi-storey structures. For such a method, a logical probabilistic design criterion

would be

$$P(E_H > E_{H\text{limit}}) \leq p_t \quad (15)$$

where the energy quantities are for the real MDOF structure and  $E_{H\text{limit}}$  and  $p_t$  are target values specified by a design code. In words, Equation (15) states that the probability of exceeding a certain limiting hysteretic energy value,  $E_{H\text{limit}}$ , should not be more than certain target value,  $p_t$ .

The UHS for normalized hysteretic energy provide information on seismic energy demand on a SDOF system (on  $E_h$ , not on  $E_H$ ). This section discusses how a design checking equation is developed for a MDOF structure (as in Equation (15)) using UHS and an equivalent system technique.

Consider the response of a SDOF oscillator, when a scale factor  $S$  is applied to the ground motion

$$\ddot{u} + 2\zeta\omega_n\dot{u} + (\omega_n)^2\gamma(\alpha_k, u) = -S\ddot{u}_g \quad (16)$$

where  $\gamma$  is a function describing the behaviour of a non-linear inelastic system with bilinear stiffness characteristics. If  $S$  is deterministic and equal to 1, then Equation (16) becomes Equation (1), which was solved for various  $d_y$  or  $C_y$  values to come up with the UHS.

Equation (16) corresponds to the response of a SDOF system when the ground motion is scaled by a factor  $S$ . It can be shown that if both the ground motion record and the yield displacement are scaled by the same factor  $S$ , then the absolute hysteretic energy ( $E_h$ ) response gets scaled by a factor  $S^2$ .

To account for the site soil effect, the factor  $F$  (Equation (14)) has to be applied to the ground acceleration. Apart from  $F$ , another ground motion scale factor  $P^*$  has to be applied to the ground acceleration while using the equivalent system (Equation (11)). Therefore, the UHS information needs to be scaled by a factor  $S = P^*F$  in order to obtain the correct ESDOF hysteretic energy response ( $E_H^*$ ):

$$E_H^* = S^2 E_h = (P^*F)^2 E_h \quad (17)$$

Using Equation (17), one can derive that when absolute energy quantities are normalized by the corresponding factors ( $kd_y^2$  and  $K^*(D_y^*)^2$ , for the SDOF and the ESDOF systems, respectively), the same normalized energy quantities are obtained for both the SDOF and ESDOF systems. However, the equivalent system does not estimate the MDOF response correctly. The hysteretic energies for the equivalent system and the MDOF structure are related by Equation (13), which can now be expressed in the form

$$E_H = N E_H^* = N (P^*F)^2 E_h = (P^*F\sqrt{N})^2 E_h \quad (18)$$

Thus, energy demand on the MDOF structure can be estimated considering a scale factor  $S = (P^*F\sqrt{N})$ . Note that,  $P^*$  is the deterministic part of the scaling factor, while  $F\sqrt{N}$  is the random part.

Response statistics from the probabilistic seismic hazard analyses, which form the basis of the UHS, were used to formulate an empirical function of  $C_y$  in Equation (7). This empirical function is now expressed as

$$Z_1(C_y) = P(E_N > E_{Nt} \text{ given } C_y \text{ for } S = 1) = \exp\{-a(C_y)^b\} \quad (19)$$

Note that  $Z_1$  is not a true cumulative distribution function, but just an expression of the probability of exceedance for some target  $E_{Nt}$ . This  $Z_1$  can also be used for expressing a probability of exceedance in terms of the hysteretic (non-normalized) energy quantity,  $E_h$ , of the SDOF:

$$Z_1(C_y) = P(E_h > kd_y^2 E_{Nt} \text{ given } C_y \text{ for } S = 1) \quad (20)$$

If  $S$  is a random variable ( $S \geq 0$ ), then it is necessary to redefine the empirical function as  $Z_S(C_y)$ , which can be related to the empirical function for  $S = 1$  (Equation (19)) by the following equation:

$$Z_S(C_y) = \int_0^\infty Z_1\left(\frac{C_y}{s}\right) f_S(s) ds \quad (21)$$

where  $f_S(s)$  is the probability density function for random variable  $S$ . This is the convolution equation with respect to  $S$ , and it represents the theorem of total probability in a continuous form [28]. The rationale behind Equation (21) has been discussed in detail by Collins [13] and Ghosh [16].

It is assumed for these uncertainty analyses that the structure is repaired back to its original 'ideal' state after the occurrence of any earthquake, along with any minor damage due to aging, strength loss due to fatigue, etc. In other words, the probability of damage due to any earthquake is independent of past events, seismic or otherwise.

Considering the deterministic part of the scale factor separately, Equation (21) is used to account for the random variable  $S$ , where  $S = F\sqrt{N}$ . Since both  $F$  and  $\sqrt{N}$  are assumed to follow lognormal distributions (refer to Section 5), their product can be treated as another lognormal random variable.

The function  $Z_S$  (Equation (21)) is an expression of probability of exceedance based on some limiting value of normalized hysteretic energy. A suitable value of the argument  $C_y$  of the function  $Z_S$  can be obtained, for which the convolution integral equals the target probability,  $p_t$ , to meet a design criterion. The following equation is solved for this purpose, considering  $F\sqrt{N}$  as the random scale factor ( $S$ ):

$$Z_{S=F\sqrt{N}}(C_y) = p_t \quad (22a)$$

$$C_y = Z_{S=F\sqrt{N}}^{-1}(p_t) \quad (22b)$$

The value of  $C_y$ , as it is evident from the above equation, depends on the target probability ( $p_t$ ), bias factor ( $N$ ) and the soil factor ( $F$ ). In addition,  $C_y$  also depends on the period ( $T$ ) and the target energy quantity ( $E_{Nt}$ ), because of the nature of probability function,  $Z_1$ , that defines the UHS. By method of trial and error, a set of  $C_y$  values is obtained, which solves Equation (22b) for different values of  $p_t$ ,  $N$ ,  $F$ ,  $T$  and  $E_{Nt}$ .

A design factor  $\Omega$  is introduced so that  $C_y$  required for certain  $p_t$  with a random scale factor  $S$ , can be obtained just by scaling the required  $C_y$  from UHS for that  $p_t$  (that is  $C_y$  for scale factor = 1). Probability information from the UHS and from Equation (22b) is combined using this factor. The factor is defined as

$$\Omega = \frac{P^* Z_S^{-1}(p_t)}{P^* f \sqrt{n} Z_1^{-1}(p_t)} = \frac{\text{Actual } C_y \text{ required for a random } S \text{ at } p_t}{\text{Estimated design } C_y \text{ at } p_t \text{ from UHS, after scaling}} \quad (23)$$

$\sqrt{n}$  and  $f$  are selected design values of the random variables  $\sqrt{N}$  and  $F$ , respectively. Note that the deterministic part ( $P^*$ ) of the scale factor cancels out, so it does not affect the value of the design factor.

Values of the design factor  $\Omega$  are calculated based on the UHS information (Equation (19)) and  $C_y$  values from Equation (22b). The design value of  $\sqrt{N}$  is selected to be its mean value. For the other random variable  $F$ , the median value (that is, the value given by Equation (14)) is selected as the design value  $f$ . Table V presents the values of the design factor  $\Omega$  for many different combinations of  $p_t$ ,  $T$  and  $E_{Nt}$ . These values are calculated assuming that the bias statistics for the three-storey building apply at all periods. This is obviously not correct, but it provides a convenient way to investigate how much  $\Omega$  varies with  $T$  and  $p_t$ . Similar tables can be found in Reference [16] that use the bias statistics for the nine- and twenty-storey buildings. Target normalized energy ( $E_{Nt}$ ) quantities of 3, 4 and 5 are selected for this calibration based on the range of  $E_N$  response of real multi-storey frames under real ground motions, which were studied for validation of equivalent system methodology. These limiting values can be related directly to parameters like 'equivalent number of yield cycles' or 'full hysteresis loops'; for example, for a ductility ( $\mu$ ) of 2,  $E_{Nt} = 4$  signifies 1 equivalent yield cycle.

It can be observed from Table V, that calibrated values of  $\Omega$  are not always reasonable. For example,  $\Omega$  attains very low values for  $p_t = 50\%$  in 50 years and low natural periods ( $T = 0.1, 0.3, 0.5$  s, etc.) for the three-storey building. The reason behind these 'odd' values of  $\Omega$  is that  $Z_1(C_y)$  (Equation (19)) does not fit the raw UHS data very well at high exceedance probability values. The function was chosen to fit the data in the low probability region which is the reason of interest for design.

Table V. Calibrated values of design factor  $\Omega$  using bias statistics for the 3-storey building (for  $v_{ref} = 540$  m/s).

$p_t$	$\Omega$ values of different periods ( $T$ )						
	$T = 0.1$ s	$T = 0.3$ s	$T = 0.5$ s	$T = 0.7$ s	$T = 1.0$ s	$T = 2.0$ s	$T = 3.0$ s
$E_{Nt} = 3$							
50% in 50 years	0.65	0.65	0.76	0.95	0.93	1.01	0.94
10% in 50 years	1.08	1.04	1.09	1.27	1.17	1.32	0.99
10% in 100 years	1.19	1.07	1.22	1.41	1.36	1.26	1.09
5% in 100 years	1.32	1.33	1.43	1.65	1.43	1.26	1.22
10% in 250 years	1.38	1.42	1.51	1.41	1.47	1.26	1.27
$E_{Nt} = 4$							
50% in 50 years	0.78	0.75	0.62	0.87	0.97	0.90	1.00
10% in 50 years	1.25	1.12	0.91	1.28	1.22	1.10	1.10
10% in 100 years	1.43	1.33	1.14	1.41	1.24	1.33	1.20
5% in 100 years	1.33	1.33	1.34	1.51	1.45	1.42	1.22
10% in 250 years	1.42	1.41	1.38	1.56	1.41	1.47	1.25
$E_{Nt} = 5$							
50% in 50 years	0.49	0.68	0.74	1.04	0.74	1.09	1.07
10% in 50 years	0.97	1.19	1.01	1.23	1.06	0.96	1.03
10% in 100 years	1.27	1.27	1.09	1.32	1.36	1.06	1.16
5% in 100 years	1.77	1.37	1.24	1.48	1.40	1.32	1.27
10% in 250 years	1.77	1.37	1.29	1.54	1.36	1.29	1.31

As noted in Section 2, for a fixed exceedance probability and period, the required yield force coefficient is a monotonically decreasing function of  $E_{Nt}$ . The actual  $C_y$  should be greater than the required minimum value of  $C_y$ , so that the energy demand is less than the actual capacity. Using the relation between  $C_y$  and  $d_y$  (Equation (5)) the governing criterion can be expressed in terms of yield displacement

$$D_y^* \geq \frac{P^*(C_y \text{ for random scale factor } S)}{(\omega^*)^2/g} = P^* g \left( \frac{T^*}{2\pi} \right)^2 Z_S^{-1}(p_t) \quad (24)$$

Recalling the fact that the equivalent system uses  $D_y^* = D_y$ , where  $D_y$  is the global yield displacement of the MDOF structure, and using Equation (23), the performance criterion is now expressed as

$$D_y \geq P^* g \left( \frac{T^*}{2\pi} \right)^2 \Omega f \sqrt{n} Z_1^{-1}(p_t) = P^* g \left( \frac{T^*}{2\pi} \right)^2 \Omega f \sqrt{n} (C_y \text{ from UHS at } p_t) \quad (25)$$

Equation (25) is a deterministic design checking equation which satisfies a probabilistic performance criterion in the form of Equation (15). The uncertainty involved in the probabilistic criterion is accounted for through the design factor  $\Omega$ . Values of such a design factor for different conditions can be provided in design codes so that the designer does not have to perform any uncertainty analysis at all. The next section illustrates how a building design is checked for a hypothetical probabilistic hysteretic energy-based performance criterion using the concept developed here.

## 7. DESIGN CHECKING EXAMPLE

In order to illustrate the procedure of design checking, a three-storey steel moment frame building is selected. The building has similar layouts in plan and elevation as the SAC three-storey building considered earlier (Figure 6). Details of the member sizes and gravity loads acting on the trial design frame are provided in Table VI. In order to use the calibrated design factor, the building is assumed to be located at the site for which the UHS are generated and the design factor is calibrated. A shear wave velocity,  $v_{\text{site}} = 540$  m/s is assumed for the same reason.

A hypothetical design criterion based on probabilistic hysteretic energy demand is chosen to illustrate how the proposed design concept can be used. The performance criterion selected for

Table VI. Details of member sizes and gravity loads applied to the trial 3-storey frame.

Storey/ floor	Columns			Point load on columns (kip)*		Distributed load on girders (k/ft)†
	Exterior	Interior	Girders	Exterior	Interior	
1/2	W14 × 311	W14 × 257	W33 × 118	23.6	34.8	1.00
2/3	W14 × 311	W14 × 257	W30 × 116	23.6	34.8	1.00
3/Roof	W14 × 311	W14 × 257	W24 × 68	20.3	30.9	0.85

There is a 4th 'pin-connected' bay on the right side of the frame, having W21 × 44 section for girders and W14 × 68 section for columns.

\*1 kip = 4.448 kN.

†1 k/ft = 14.59 kN/m.

this building is to limit the exceedance probability ( $p_t$ ) to 10% in 50 years for a target normalized hysteretic energy ( $E_{Nt}$ ) of 4. The selected trial design is known to have satisfied the 'strong-column-weak-beam' mechanism condition in non-linear pushover analysis under the UBC lateral force distribution [25].

The design checking steps are as follows:

1. Perform a pushover analysis of the frame.
2. Obtain the structural response ( $D_y$ , etc. for the equivalent system scheme).
3. Calculate ESDOF parameters from pushover results (Equations (10) and (11)).
4. Obtain the design soil factor from Equation (14) (using  $v_{ref} = 540$  m/s).
5. Obtain the design bias factor for the frame from Table IV.
6. Obtain the design factor for the given condition from Table V.
7. Obtain the yield force coefficient from the UHS for given  $E_{Nt}$ ,  $T$  and  $p_t$ .
8. Check actual  $D_y$  (Step 2) against the minimum required from Equation (25).

The sample design is checked following these steps:

1. In order to obtain the ESDOF parameters for the frame (following the *virtual work formulation*) a pushover analysis is carried out up to 2.5% global drift using the UBC lateral force distribution:  $\{f\}^T = \{0.52, 0.32, 0.16\}$  (from top to bottom).
2. The pushover analysis yields the following:  $\Delta_y = 9.75 \times 10^{-3}$ ;  $D_y = 4.56$  in (116 mm);  $V_y = 958$  kips (4261 kN);  $\{\Phi_1\}^T = \{1.0, 0.665, 0.273\}$  (based on displacement profile at  $\Delta = 1\%$ );  $\{\Phi_2\} = \{\Phi_1\}$ .
3. ESDOF parameters are calculated:  $M^* = \{\Phi_2\}^T [M] \{\Phi_1\} = 4.37$  kip-s<sup>2</sup>/in (7.65 kN-s<sup>2</sup>/mm);  $L^* = \{\Phi_2\}^T [M] \{1\} = 5.52$  kip-s<sup>2</sup>/in (9.67 kN-s<sup>2</sup>/mm);  $P^* = L^*/M^* = 1.26$ ;  $\omega^* = 6.11$  rad/s<sup>2</sup>;  $T^* = 1.03$  s;  $K^* = 163$  kip/in (285 kN/mm).
4. From Equation (14), for  $v_{site} = 540$  m/s:  $f = 1.0$ .
5. From Table IV, for three-storey building:  $\sqrt{n} = 1.09$ .
6. From Table V, for three-storey building,  $E_{Nt} = 4$ ,  $p_t = 10\%$  in 50 years,  $T^* = 1.03$  s (using  $T^* = 1.0$  s):  $\Omega = 1.23$ .
7. From UHS plots, for  $E_{Nt} = 4$ ,  $p_t = 10\%$  in 50 years,  $T^* = 1.03$  s (using  $T^* = 1.0$  s):  $C_y = 0.25$ .
8. Inserting the values in Equation (25):

$$D_y \geq 1.26 \times 386.4 \times \left(\frac{1.03}{2\pi}\right)^2 \times 1.23 \times 1.0 \times 1.09 \times (0.25) \text{ in} = 4.43 \text{ in (113 mm)}$$

The actual  $D_y$ , from Step 2 (4.56 in = 116 mm), is more than the minimum required. Therefore, the trial design satisfies the performance criterion.

## 8. CONCLUSIONS

A concept of developing a probabilistic hysteretic energy-based design checking methodology is explored in this paper. The concept discussed here merges the idea of considering energy as a demand parameter into a framework of reliability-based seismic design for building structures. This proposed design checking concept is consistent with the concept for an energy-based

performance-based design methodology as proposed by the Vision 2000 Committee [1] because it explicitly considers a probabilistically defined criterion for the building performance (not just the hazard level) in terms of an energy parameter.

The advantage of the proposed design checking format is that it eliminates the need of any uncertainty analysis from the designer's part as the design criterion is checked only with a deterministic equation. Also, there is no need for the designer to perform any non-linear dynamic analysis; a non-linear static pushover analysis is sufficient.

Although the concept presented herein is a significant first step toward an energy-based, reliability-based design procedure, it is recognized that more work is needed to refine the concept and to address some remaining issues. Some important topics requiring further study are as follows:

- The methods to quantify structural damage in terms of energy demand (or any derived demand parameter) have not been standardized yet. It is unclear which energy demand parameter is best suited for this purpose, and also what value of the chosen parameter corresponds to a specific performance level. These issues are beyond the scope of this article, and detailed analytical and experimental research is needed to resolve these issues.
- It has been argued elsewhere that the effects of pulse-type near-fault ground motions are hidden in UHS and that there exists a need to consider these near-fault ground motions separately [29]. However, the goal of a probabilistic hazard analysis is not to put emphasis on certain specific earthquake(s) only because of its huge damaging capability, unless such an earthquake has high frequency of occurrence at the specific site under consideration. A PSHA to construct UHS emphasizing the effects of near-fault motions is an issue to be addressed by seismologists and engineers working together.
- The calculations presented herein are based on UHS derived from time-intensive simulation procedures for only one specific site. In practice, it will be necessary to obtain UHS information based on hazard maps for an entire region or country. Such issues, related to probabilistic hazard estimation and presentation of the results in a format suitable for code implementation, need detailed exploration.
- The results presented herein clearly show that the ESDOF methodology does a better job of predicting energy demand for a low-rise building than it does for mid- to high-rise buildings. Further research work is needed in order to optimize the ESDOF methodology or to explore alternative techniques [16–18, 20, 30].
- Values of the design factor need to be calibrated for other building systems and different locations, following the techniques adopted herein, to check if design codes will be able to specify 'standard' values for use in design.
- It should also be noted that the proposed concept is not a true 'design' methodology but is a design checking technique. A method of obtaining actual member sizes to satisfy certain yield displacement criterion will be a goal of future modifications of the current work.

#### ACKNOWLEDGEMENTS

Partial support for this research was provided by the U.S. National Science Foundation (NSF) through the Grant CMS-9721452. The findings and opinions expressed herein are those of the authors and do not necessarily represent the views of NSF. The authors would like to thank the reviewers of the manuscript for their time and valuable insights and suggestions.

## REFERENCES

1. Structural Engineers Association of California (SEAOC) VISION 2000 Committee. *Performance Based Seismic Engineering of Buildings*, vol. 1. SEAOC: Sacramento, CA, 1995.
2. Housner GW. Limit design of structures to resist earthquakes. *1st World Conference of Earthquake Engineering, Proceedings*. EERI: Berkeley, CA, 1956.
3. Zahrah TF, Hall WJ. Earthquake energy absorption in SDOF structures. *Journal of Structural Engineering (ASCE)* 1984; **110**(8):1757–1772.
4. Uang C-M, Bertero VV. Use of energy as a design criterion in earthquake-resistant design. *Report No. UCB/EERC-88/18*, University of California at Berkeley, CA, 1988.
5. Fajfar P. Equivalent ductility factors, taking into account low-cycle fatigue. *Earthquake Engineering and Structural Dynamics* 1992; **21**:837–848.
6. Bertero RD, Bertero VV, Teran-Gilmore A. Performance-based earthquake-resistant design based on comprehensive design philosophy and energy concepts. Paper No. 611, *11th World Conference on Earthquake Engineering, Proceedings*. Elsevier: Amsterdam, 1996.
7. Riddell R, Garcia JE. Hysteretic energy spectrum and damage control. *Earthquake Engineering and Structural Dynamics* 2001; **30**:1791–1816.
8. Chou C-C, Uang C-M. Establishing absorbed energy spectra—an attenuation approach. *Earthquake Engineering and Structural Dynamics* 2000; **29**:1441–1455.
9. Manfredi G. Evaluation of seismic energy demand. *Earthquake Engineering and Structural Dynamics* 2001; **30**:485–499.
10. Park YJ, Ang AH-S. Mechanistic seismic damage model for reinforced concrete. *Journal of Structural Engineering (ASCE)* 1985; **111**(4):722–739.
11. Chopra AK. *Dynamics of Structures: Theory and Applications to Earthquake Engineering*. Prentice Hall: Englewood Cliffs, NJ, 1995.
12. Housner GW. Measures of severity of earthquake ground shaking. *1st US National Conference on Earthquake Engineering, Proceedings*, Ann Arbor, MI, 18–20 June, 1975.
13. Collins KR. Investigation of alternative seismic design procedures for standard buildings. *Ph.D. Thesis*, Department of Civil Engineering, University of Illinois at Urbana-Champaign, IL, 1995.
14. Collins KR, Wen YK, Foutch DA. Dual-level seismic design: a reliability based methodology. *Earthquake Engineering and Structural Dynamics* 1996; **25**:1433–1467.
15. Building Seismic Safety Council (BSSC). *NEHRP Recommended Provisions for the Development of Seismic Regulations for New Buildings*, Volume 1 & 2, Washington, DC, 1992.
16. Ghosh S. Two alternatives for implementing performance-based seismic design of buildings—life cycle cost and seismic energy demand. *Ph.D. Thesis*, Department of Civil Engineering, University of Michigan, Ann Arbor, MI, 2003.
17. Qi X, Moehle JP. Displacement design approach to reinforced concrete structures subjected to earthquakes. *Report No. UCB/EERC-91/02*, University of California at Berkeley, CA, 1991.
18. Nassar AA, Osteraas JD, Krawinkler H. Seismic design based on strength and ductility demands. *10th World Conference on Earthquake Engineering, Proceedings*, vol. 10, Madrid, Spain, 19–24 July 1992; 5861–5866.
19. Lawson RS, Vance V, Krawinkler H. Non-linear static pushover analysis—why, when and how? *5th US National Conference on Earthquake Engineering, Proceedings*, vol. 1. Chicago, IL, 10–14 July 1994; 283–292.
20. Chen P-T. Investigation of pushover analysis procedure for reliability-based and performance-based seismic design with applications to asymmetric building structures. *Ph.D. Thesis*, Department of Civil Engineering, University of Michigan, Ann Arbor, MI, 1999.
21. Blume JA. A reserve energy technique for the earthquake design and the rating of structures in the inelastic range. *2nd World Conference on Earthquake Engineering, Proceedings*, Tokyo and Kyoto, Japan, 11–18 July 1960; 1061–1083.
22. Clough RW, Penzien J. *Dynamics of Structures*. McGraw-Hill: New York, 1975.
23. Gupta A, Krawinkler H. Seismic demands for performance evaluation of steel moment resisting frame structures (SAC Task 5.4.3). *Report No. 132*, John A. Blume Earthquake Engineering Center, Department of Civil and Environmental Engineering, Stanford University, Stanford, CA, 1999.
24. RAM International. *RAM Perform 2D: User Guide*, Version 1.0, Carlsbad, CA, 2000.
25. International Conference of Building Officials (ICBO). *Uniform Building Code*. ICBO: Whittier, CA, 1997.

26. Borchardt RD. New development in estimating site effects on ground motion. *Seminar on New Development in Earthquake Ground Motion Estimation and Implications for Engineering Design Practice, Proceedings*, Chapter 10, ATC 35-1, Redwood City, CA, 1994.
27. Borchardt RD. Estimates of site-dependent response spectra for design (methodology and justification). *Earthquake Spectra* 1994; **10**(4):617–653.
28. Ang AH-S, Tang WH. *Probability Concepts in Engineering Planning and Design: Volume 1. Basic Principles*. Wiley: New York, 1975.
29. Krawinkler H. Challenges and progress in performance-based earthquake engineering. *International Seminar for Seismic Engineering for Tomorrow—In Honor of Professor Hiroshi Akiyama*, Tokyo, Japan, 1999.
30. Estes KR, Anderson JC. Hysteretic energy demands in multistory buildings. *7th US National Conference on Earthquake Engineering, Proceedings*, Boston, MA, 21–25 July 2002.